J. Fluid Mech. (2004), *vol.* 502, *pp.* 199–206.
DOI: 10.1017/S0022112003007717 Printed in the United Kingdom

Flat-plate aerodynamics at very low Reynolds number

By QUANHUA SUN AND IAIN D. BOYD

Department of Aerospace Engineering, University of Michigan, Ann Arbor, MI 48109, USA

(Received 28 July 2003 and in revised form 7 December 2003)

Gas flow over a flat-plate airfoil at very-low Reynolds number is investigated in order to understand the aerodynamic issues related to micro air vehicle design and performance. Studies have shown that such low Reynolds number flow exhibits rarefied phenomena and a flat plate having a thickness ratio of 5% has better aerodynamic performance than conventional streamlined airfoils. This paper simulates air flows over a 5% flat plate using a hybrid continuum–particle approach for flows having a Mach number of 0.2 and a Reynolds number varying between 1 and 200. Investigation shows that low Reynolds number flows are viscous and compressible, and rarefied effects increase when the Reynolds number decreases. It is also found that there is a minimum lift slope for the plate airfoil at a Reynolds number near 10 and the drag coefficient monotonically increases with decreasing Reynolds number.

1. Introduction

There is increasing interest in designing aircraft that are as small as possible for special military and civil missions (Mueller 2001). Many such aircraft are currently under development, including micro-sized unmanned aerial vehicles and micro air vehicles. However, research and development at significantly smaller scales (corresponding to very low Reynolds number flows) is still in its infancy. There are very few computations and experiments for aerodynamics of airfoils at Reynolds number (Re) below 1000. The objectives of this paper are to understand external flows at low Reynolds number and to investigate the aerodynamics of a flat-plate airfoil at Reynolds number below 1000.

The dependence of airfoil performance on the flow Reynolds number is well known. When $Re > 10^6$, the variation of airfoil characteristics with the Reynolds number is rather slow (Jones 1990). However, when the Reynolds number is on the order of 10^5, the aerodynamics of airfoils varies rapidly with their configuration. Schmitz (see Jones 1990) performed a careful experimental study of the behaviour of airfoils in the low range of Reynolds number. The experiments showed that a thin flat plate is inferior to a conventional shaped airfoil when $Re = 1.2 \times 10^5$, but superior when $Re = 4 \times 10^4$. Sunada, Sakaguchi & Kawachi (1997) compared the aerodynamics of several airfoils when $Re = 4 \times 10^3$ by towing them through water in a tank. They concluded that a flat plate with a thickness ratio of 5% has larger lift slope than conventional streamlined airfoils.

It is also found that the properties of low Reynolds number flows depend on the Mach number (Ma) (Sun 2003). The drag on a micro-scale flat plate was studied using both the direct simulation Monte Carlo (DSMC) method (Bird 1994) and the information preservation (IP) method (Sun & Boyd 2002). It was concluded

based on the numerical results and experimental data (Schaaf & Sherman 1954) that the normalized drag coefficient ($C_D Ma$) on flat plate depends on a combination of Reynolds and Mach numbers ($\sqrt{Re}/Ma^{0.8}$) when this combination is between 1 and 100, which clearly demonstrates the compressible effects for low Reynolds number flows.

Low Reynolds number flows also exhibit rarefied effects because an important rarefied parameter, the Knudsen number (Kn), is inversely proportional to the Reynolds number when the Mach number remains unchanged. Hence, continuum equations, e.g. the Navier–Stokes equations, are physically invalid for very low Reynolds number flows, and kinetic-based approaches are therefore preferred to simulate these flows. Recently, Sun, Boyd & Candler (2002) simulated the flow over a flat-plate airfoil at a Reynolds number of 4.0 using both the kinetic-based and continuum-based approaches, and showed that continuum approaches solving the Navier–Stokes equations are not physically appropriate.

Kinetic methods, however, are generally several orders of magnitude more numerically expensive than continuum-based computational fluid dynamic techniques. Therefore, an efficient approach is to combine the numerical efficiency of a continuum approach for the continuum region and the physical accuracy of a kinetic approach for the rarefied region in the computational domain. Sun, Boyd & Candler (2003) developed such a hybrid approach suitable for subsonic, micro-scale gas flows by strongly coupling a Navier–Stokes solver and the information preservation method. In the hybrid approach, the entire computational domain is divided into continuum domains and particle domains using an interface that is adaptively determined by a continuum breakdown parameter. The continuum domain is solved using a Navier–Stokes approach and the particle domain is simulated using the IP method, while necessary information is exchanged through the interface at every time step.

In this paper, we simulate air flows over a 5% flat-plate and investigate the aerodynamics of this flat-plate airfoil at a Reynolds number in the range $1 < Re < 200$ when the free-stream Mach number is 0.2 using the hybrid continuum–particle approach. The Reynolds number here is defined at the free-stream conditions with the use of the plate length. Details on the computation are described in § 2, and numerical results are presented in § 3 along with related experimental and theoretical data. Finally, we summarize the major conclusions of this study in § 4.

2. Computational framework for simulating flow over a flat-plate airfoil

Air flows over a flat-plate airfoil at low Reynolds number are simulated using the hybrid continuum–particle approach (Sun *et al.* 2003). The airfoil is a 30-micron-long flat plate having a thickness ratio of 5%. The plate is kept at a temperature of 295 K, and full momentum accommodation is assumed. The free stream has a Mach number of 0.2 and a temperature of 295 K. Three free-stream pressures are considered in this investigation: 1.0 atm, 0.1 atm, and 0.01 atm. The corresponding Reynolds numbers are calculated as 135.7, 13.57, and 1.357 using expression $Re = \rho_\infty V_\infty L/\mu_\infty$, where ρ_∞ is the free-stream density, V_∞ is the free-stream velocity, L is the length of the plate, and μ_∞ is the viscosity coefficient of air at the free-stream temperature.

The computational domain has an area with a radius of 150 microns and uses characteristic boundary conditions. The computational cells are clustered around the flat plate, especially near the leading and trailing edges. The cell size is less than the mean free path of air molecules for cells near the plate, and increases for cells away from the plate where the gradients of local flow properties are large. However,

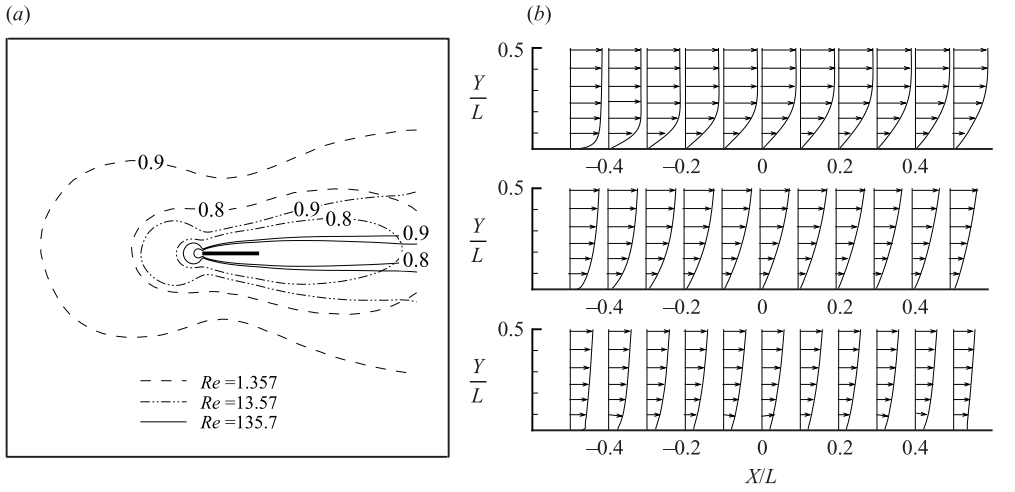

FIGURE 1. Viscous effects on velocity profiles. (*a*) Velocity contours when $|V|/V_\infty = 0.8$ and 0.9. (*b*) Parallel velocity profiles above the plate (top: $Re = 135.7$; middle: $Re = 13.57$; bottom: $Re = 1.357$).

the cell size of continuum cells does not need to be less than the mean free path of air molecules. The total number of computational cells is 21300 when $Re = 135.7$, 14200 when $Re = 13.57$, and 5100 when $Re = 1.357$. Grid convergence studies were performed to verify that the results are grid independent.

When $Re = 135.7$, the computational domain is divided by a fixed interface, in which the particle domain is set larger than that indicated by the continuum breakdown parameter $B = 0.005$ (Sun *et al.* 2003). Hence, the Navier–Stokes solver and the slip velocity model are valid for the determined continuum domain. However, when the Reynolds number is smaller, the hybrid approach is only used for the flow to reach a steady state, and thereafter the entire computational domain is simulated using the IP method.

3. Numerical results and discussion

3.1. *Viscous effects*

The Reynolds number denotes the ratio of the inertia force to the viscous force. Hence, viscous effects are important when the flow Reynolds number is small. For flow over the flat-plate airfoil, when gas molecules hit the plate surface, they are accommodated to the plate velocity. These molecules then collide with nearby molecules due to their thermal movement, and affect the flow field at a distance of the order of one mean free path around the plate airfoil. As a result, a low Reynolds number flow is slowed down to a large extent and the boundary layer is thickened, while the leading and trailing edges affect a significant fraction of the plate length.

The velocity (V) contours for $|V|/V_\infty = 0.8$ and 0.9 are shown in figure 1(*a*) for all three cases when the angle of attack (α) is zero. The flat plate slows the flow and this effect increases when the Reynolds number decreases. The parallel velocity profile of the flow above the flat plate is shown for the three cases in figure 1(*b*) where the velocity scale is the same for all cases and X, Y are the coordinates parallel and perpendicular to the plate, respectively. When $Re = 135.7$, the velocity follows a typical laminar boundary layer profile. However, the thickness of the boundary layer

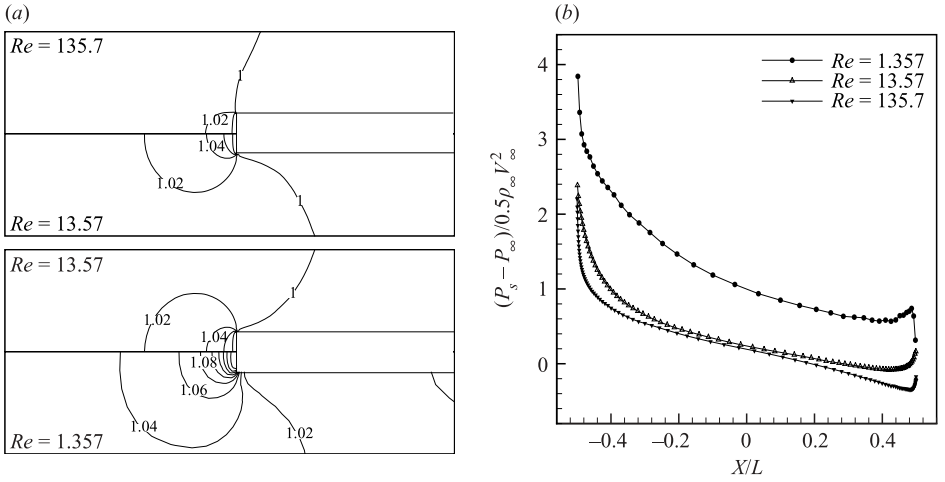

FIGURE 2. Reynolds number effects on the compressibility of the gas flow. (*a*) Density flow field ρ/ρ_∞. (*b*) Pressure coefficient distribution on the lower side of the plate when $\alpha = 20°$.

becomes very large for the cases with lower Reynolds number (if the concept of the boundary layer can still be used) although there is obvious velocity slip on the plate surface.

3.2. *Compressible effects*

It is generally assumed that a flow is incompressible when the flow Mach number is below 0.3. However, a flow becomes compressible at a low Reynolds number even when the Mach number of the flow is small. If the isentropic assumption is followed, the density variation is within 2% when $Ma = 0.2$. Figure 2(*a*) shows that the density variation increases when the Reynolds number decreases, and the variation can be as high as 16% when $Re \approx 1$, which indicates that the isentropic assumption is invalid because the flow is rarefied. The Reynolds number effects on the compressibility of a flow can also be found on the pressure $(P_s - P_\infty)/0.5\rho_\infty V_\infty^2$ coefficient distributions that are shown in figure 2(*b*) for the distributions on the lower side of the plate when $\alpha = 20°$. It is found that the pressure coefficient for the case with $Re = 13.57$ is very close to that when $Re = 135.7$, which may indicate that this effect is not significant when the Reynolds number is above 10. However, there are very large differences between the pressure coefficients when the Reynolds number is 1.357 and 13.57. This is not surprising because free molecular theory predicts an even larger pressure coefficient.

3.3. *Rarefied effects*

A velocity slip exists on the solid surface for flows in the slip regime where the Knudsen number (the ratio of the mean free path of gas molecules to the smallest characteristic length of the flow) is between 0.01 and 0.1. However, this Knudsen number range is only conceptual because the smallest characteristic length is not well defined.

The slip velocity (V_s) on the upper side of the plate is shown in figure 3(*a*) for three cases when $\alpha = 0°$. It shows that there is a considerable amount of velocity slip near the leading edge, although the global Knudsen number based on the plate length is only about 0.002 when $Re = 135.7$. It is also found that the slip velocity increases when the Reynolds number decreases. These results show that the rarefied

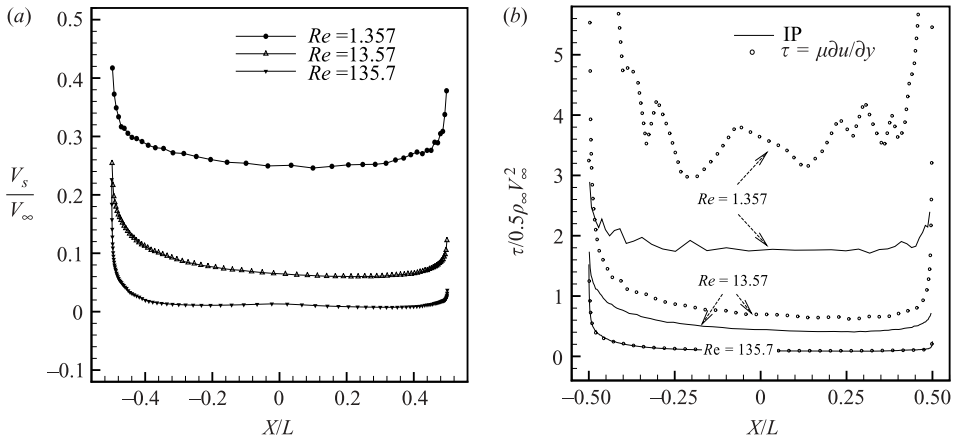

FIGURE 3. Reynolds number effects on the rarefaction of the gas flow. (*a*) Slip velocity on the upper side of the plate. (*b*) Comparison of skin friction coefficient on the upper side of the plate when $\alpha = 0°$.

effect exists only near the leading edge when the Reynolds number is not too small and the effect expands to larger domains when the Reynolds number decreases.

It is interesting to see whether the linear expression for the shear stress $\tau = \mu\partial u/\partial y$ is still valid. Figure 3(*b*) compares the friction coefficient obtained from this expression and that obtained directly from the present simulation. The fluctuation of the results when $Re = 1.357$ is due to the statistical scatter associated with the IP method, which can be decreased by increasing the sample size of simulated particles. The comparison shows that the agreement is very good when $Re = 135.7$ and the linear expression gives larger shear stress when the Reynolds number is small, which indicates that continuum equations are invalid for describing very low Reynolds number flows.

3.4. *Effects of angle of attack*

Flows over the plate airfoil are simulated for angle of attack up to 50°. Figure 4 shows the pressure (P/P_∞) field and some streamlines around the airfoil for selected cases. The flow patterns when $Re = 135.7$ are illustrated in figures 4(*a*)–4(*f*). Clearly, the pressure increases where the flow reaches the leading-edge of the airfoil, and drops where the flow leaves the airfoil. There is no flow separation when $\alpha \leqslant 10°$. However, when $\alpha = 20°$, the flow begins to separate near the upper leading edge because of the strong local adverse pressure gradient. When $\alpha = 30°$, another separation occurs near the trailing edge of the plate. The flow is then dominated by the two separation regions or two vortices. The downstream vortex becomes stronger when the angle of attack increases ($\alpha = 40°$), and this vortex almost consumes the upstream vortex when $\alpha = 50°$.

The flow patterns when $Re = 13.57$ and 1.357 exhibit different flow behaviour than for $Re = 135.7$. Apart from the phenomena already mentioned, there are several new effects. First, flow separation is delayed and weakened (figures 4*g* and 4*h*) when the Reynolds number decreases. There is no separation when $Re = 1.357$ for angle of attack up to 50° (figures 4*i*). Second, the pressure gradient near the leading edge decreases although the overall pressure variation increases when the Reynolds number decreases. Therefore, it can be anticipated that the aerodynamics of the plate airfoil at very low Reynolds number are very different from those at more usual Reynolds numbers.

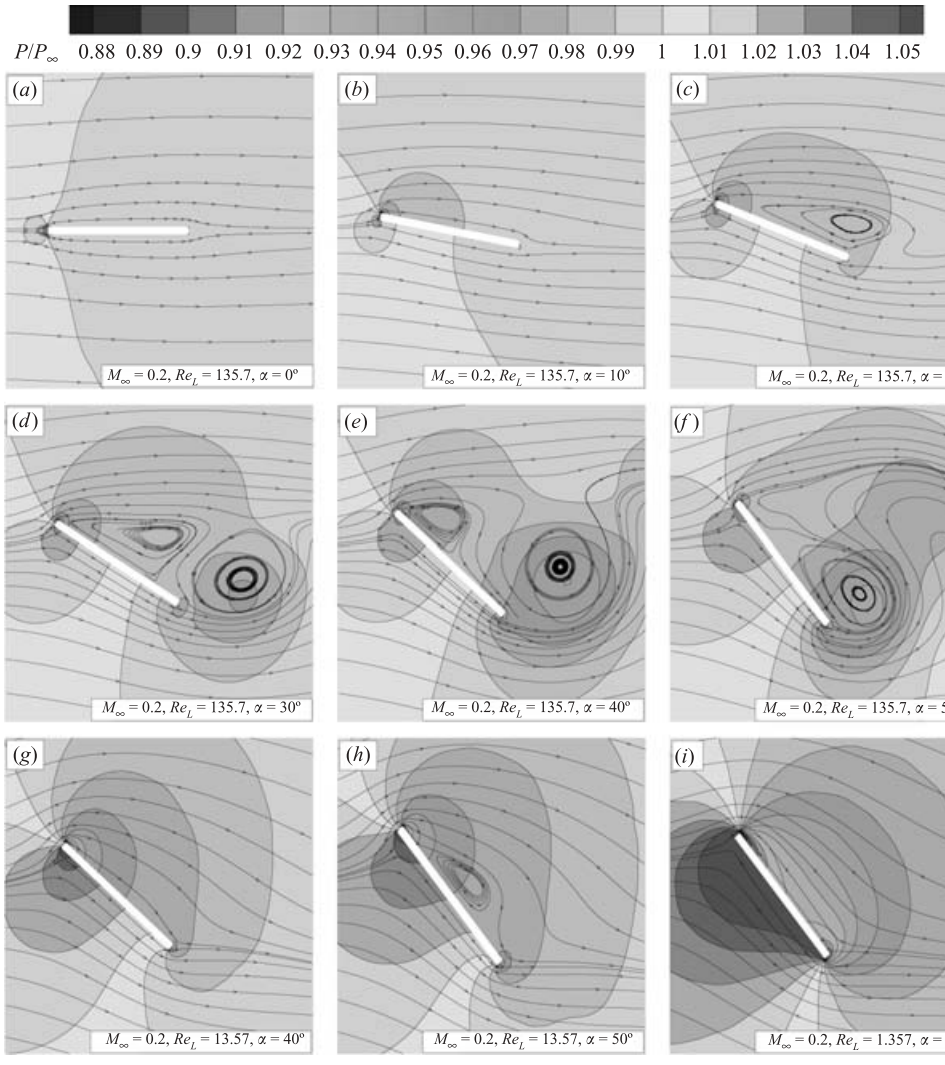

FIGURE 4. Pressure flow field and streamlines for flows over a 5% flat plate for selected cases.

3.5. *Aerodynamic characteristics of the 5% flat plate at very low Reynolds numbers*

Airfoil theory for inviscid flow indicates that the lift slope for a thin airfoil is 2π. However, the lift slope decreases with the flow Reynolds number for conventional streamlined airfoils when $10^3 < Re < 10^7$ (Sunada *et al.* 1997). In this subsection, we compare the aerodynamics of a 5% flat plate from experiments, numerical simulations, and free molecular theory under several Reynolds number conditions.

Sunada *et al.* (1997) conducted experiments on a 5% flat plate at the chord Reynolds number of 4000 by towing the airfoil through water in a tank. Their experimental data are plotted in figure 5(*a*). It was estimated that the experimental error is within 18% for the lift and drag coefficients. The figure shows that the lift slope is 5.8 and the drag coefficient is less than 0.1 at small angle of attack.

The lift and drag coefficients calculated for the current simulations are plotted in figures 5(*b*)–5(*d*). Figure 5(*b*) shows the results when $Re = 135.7$. The lift slope is about 3.0 and the drag coefficient is roughly 0.4 at small angle of attack. The lift does

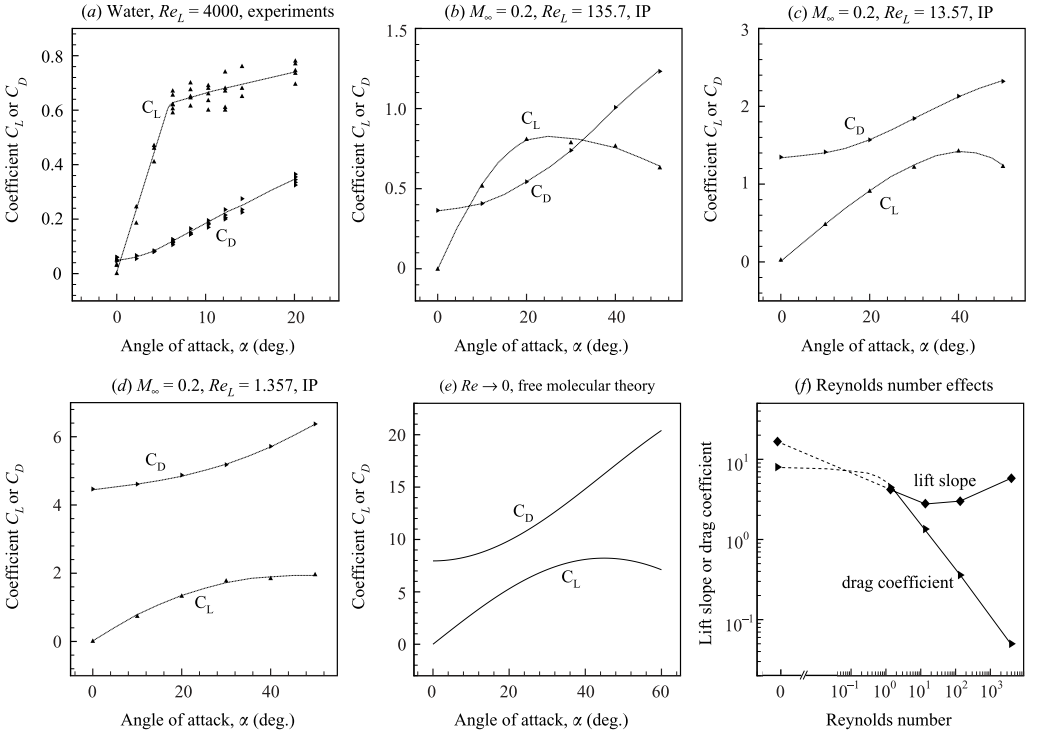

FIGURE 5. Aerodynamics of the 5% flat-plate airfoil. (*a*) Experimental data of Sunada *et al.* (1997) when $Re = 4000$; (*b*) simulation results when $Re = 135.7$ and $Ma = 0.2$; (*c*) simulation results when $Re = 13.57$ and $Ma = 0.2$; (*d*) simulation results when $Re = 1.357$ and $Ma = 0.2$; (*e*) results predicted by free molecular theory; (*f*) Reynolds number effects on the aerodynamics.

not increase linearly because the flow is separated when the angle of attack is 20° or larger. Figure 5(*c*) shows the results when $Re = 13.57$. Here, the lift slope is about 2.8 and the drag coefficient is a little larger than 1 at small angle of attack. In addition, the ratio of lift to drag is less than 1 because of the large drag coefficient. Figure 5(*d*) shows the results when $Re = 1.357$. It is found that the lift slope is about 4.2 and the drag coefficient is larger than 4.

We also calculate the lift and drag coefficients of the 5% flat plate under the free molecular condition using the following equations, derived from the free molecular theory (Gombosi 1994).

$$C_L = \cos\alpha \left[\frac{\mathrm{erf}(s\sin\alpha)}{s^2} + \sqrt{\pi}\frac{\sin\alpha}{s}\right] - 0.05\sin\alpha \left[\frac{\mathrm{erf}(s\cos\alpha)}{s^2} + \sqrt{\pi}\frac{\cos\alpha}{s}\right], \quad (3.1)$$

$$C_D = \frac{2}{\sqrt{\pi}}\left[\frac{\exp(-s^2\sin^2\alpha)}{s} + \sqrt{\pi}\sin\alpha\left(1+\frac{1}{2s^2}\right)\mathrm{erf}(s\sin\alpha) + \pi\frac{\sin^2\alpha}{2s}\right]$$
$$+ 0.05\frac{2}{\sqrt{\pi}}\left[\frac{\exp(-s^2\cos^2\alpha)}{s} + \sqrt{\pi}\cos\alpha\left(1+\frac{1}{2s^2}\right)\mathrm{erf}(s\cos\alpha) + \pi\frac{\cos^2\alpha}{2s}\right], \quad (3.2)$$

where $s = \sqrt{V_\infty^2/(2RT)}$. Figure 5(*e*) shows that the lift slope is as high as 16.5 and the drag coefficient is larger than 7.9. The ratio of lift to drag, however, is less than 1.

The Reynolds number effects on the lift slope and the minimum drag coefficient of the plate airfoil are illustrated in figure 5(*f*). The results show that there is a minimum

lift slope at a Reynolds number near 10 for the aerodynamic characteristics of the airfoil, while the drag coefficient monotonically increases when the Reynolds number decreases.

4. Conclusions

The aerodynamics of a 5% flat-plate airfoil at Reynolds numbers below 1000 were investigated using a hybrid continuum–particle approach.

Studies showed that very low Reynolds number flows are very different from high Reynolds number flows. First, the viscous force dominates very low Reynolds number flows. The leading and trailing edges affect a significant fraction of the plate length. The boundary layer equations are clearly inappropriate. The flow around the plate is severely slowed and the skin friction coefficient is very large when the Reynolds number is small. Second, very low Reynolds number flows are compressible. The pressure coefficient increases when the Reynolds number decreases. The density variation can be as high as 15% of the density of the free stream having a Mach number of 0.2 when the Reynolds number is about 1. Hence, the incompressible assumption is generally invalid for gas flows at very low Reynolds numbers. Third, rarefied effects become important for very low Reynolds number flows. Rarefied phenomena start to appear near the leading and trailing edges and expand to domains around the airfoils when the Reynolds number decreases. Therefore, continuum equations cannot describe the whole flow.

The aerodynamic characteristics of the 5% flat plate are poor at very low Reynolds numbers. First, the ratio of lift to drag drops below 1 when the Reynolds number is less than 50. Second, the drag coefficient monotonically increases when the Reynolds number decreases. Third, there is a minimum lift slope of about 2.8 for the plate airfoil at a Reynolds number near 10.

The authors greatly appreciate the support from the Air Force Office of Scientific Research through MURI grant F49620-98-1-0433.

REFERENCES

Bird, G. A. 1994 *Molecular Gas Dynamics and the Direct Simulation of Gas Flows*. Oxford Science Publications.

Gombosi, T. I. 1994 *Gaskinetic Theory*. Cambridge University Press.

Jones, R. T. 1990 *Wing Theory*. Princeton University Press.

Mueller, T. J. (ed.) 2001 *Fixed and Flapping Wing Aerodynamics for Micro Air Vehicle Applications*. Progress in Astronautics and Aeronautics, vol. 195. AIAA.

Schaaf, S. A. & Sherman, F. S. 1954 Skin friction in slip flow. *J. Aeronaut. Sci.* **21**, 85–90.

Sun, Q. 2003 Information preservation methods for modeling micro-scale gas flows. PhD thesis, University of Michigan, Ann Arbor.

Sun, Q. & Boyd, I. D. 2002 A direct simulation method for modeling microscale gas flows. *J. Comput. Phys.* **179**, 400–425.

Sun, Q., Boyd, I. D. & Candler, G. V. 2002 Numerical simulation of gas flow over micro-scale airfoils. *J. Thermophys. Heat Transfer* **16**, 171–179.

Sun, Q., Boyd, I. D. & Candler, G. V. 2003 A hybrid continuum/particle approach for micro-scale gas flows. In *Rarefied Gas Dynamics* (ed. A. Ketsdever & E. Muntz). AIP Conference Proceeding, vol. 663, pp. 752–759.

Sunada, S., Sakaguchi, A. & Kawachi, K 1997 Airfoil section characteristics at a low Reynolds numbers. *Trans. ASME: J. Fluids Engng* **119**, 129–135.